Pyridine Adducts of Nickel(II) Xanthates as Single-Source Precursors for the Aerosol-Assisted Chemical Vapor Deposition of Nickel Sulfide

Naveed Alam,[†] Michael S. Hill,*[,‡] Gabriele Kociok-Köhn,[‡] Matthias Zeller,[§] Muhammad Mazhar,*[,†] and Kieran C. Molloy*[,‡]

Department of Chemistry, University of Bath, Claverton Down, Bath BA2 7AY, United Kingdom, Department of Chemistry, Quaid-I-Azam University, Islamabad 45320, Pakistan, and Department of Chemistry, Youngstown State University, 1 University Plaza, Youngstown, Ohio 44555-3663

Received May 20, 2008. Revised Manuscript Received July 22, 2008

Compounds of the type $[Ni(S_2CO^nBu)_2 \cdot (py)_2]$ (py = pyridine derivative) have been synthesized and studied as single-source precursors for the fabrication of phase-pure thin films of rhombohedral (Millerite) NiS by aerosol-assisted chemical vapor deposition. The films have been characterized by XRD, SEM, EDX, and AFM and have been found to display a substrate-dependent morphology that is effectively independent of the precise identity of the precursor complex, regardless of minor variations in thermal stability.

1. Introduction

Existing in a variety of compositions, including Ni_3S_2, Ni_6S_5, Ni_7S_6, Ni_3S_4, and NiS,[1] nickel sulfides are potentially important materials in a diverse number of technical applications. In heterogeneous catalysis, nickel sulfide nanoparticles have been reported as highly active hydrodesulfurization catalysts and,[2] when supported on γ-alumina, as catalysts for the autothermal reforming of methane for hydrogen production.[3] Phase-pure semiconducting NiS has a narrow band gap of *ca*. 0.3 eV and has thus found a number of applications in IR detection,[4,5] as a selective solar coating, and as an electrode in photoelectrochemical storage devices.[6] Although several routes to nanoparticulate NiS and the fabrication of thin film NiS by soft solution methods have been described,[7−16] there are only limited reports of the deposition of NiS either by dual- or single-source chemical vapor deposition (CVD) methods. O'Brien has recently reported the growth of thin films of binary nickel sulfide by both low pressure (LP) and aerosol-assisted (AA) CVD methods employing single source dithiocarbamate $Ni(S_2CNRR')_2$ (RR′ = EtEt, MeEt, Me^{n}Bu, or Me^{n}Hex) precursors.[17,18] Under both regimes, the phases of the films deposited on glass substrates at relatively low growth temperatures were found to be mixtures of $NiS_{1.03}$, NiS_2, NiS, and α-Ni_7S_6 and displayed a variety of morphologies that were dependent upon the alkyl substituent of the dithiocarbamate. Of more relevance to the current study is an earlier report by Zink of the low pressure laser-driven photo and thermal CVD of NiS utilizing nickel(II) isopropyl xanthate, $[Ni(S_2CO^iPr)_2]$, as a single source precursor in which notably low deposition temperatures (350 °C) resulted in high-purity films with low carbon contamination.[19] Although transition metal xanthates (or alkyldithiocarbonates) constitute a well-explored class of coordination complex,[20] their use as precursors to solid-state sulfide materials is rather underexploited.[21−23] Xanthate complexes such as $Ni(S_2CO^iPr)_2$ typically decompose by the Chugaev elimination reaction in which an alkene is formed by a concerted syn-elimination

* Corresponding author. E-mail: m.s.hill@bath.ac.uk (M.S.H.).
† Quaid-I-Azam University.
‡ University of Bath.
§ Youngstown State University.

(1) Greenwood, N. N.; Earnshaw, A. *Chemistry of the Elements*, 2nd ed.; Elsevier: Amsterdam, 1997.
(2) Neurock, M.; Van Santen, R. A. *J. Am. Chem. Soc.* **1994**, *116*, 4427.
(3) Hoang, D. L.; Chan, S. H.; Ding, O. L. *J. Power Sources* **2006**, *159*, 1248.
(4) Okamura, H.; Naitoh, J.; Nanba, T.; Matoba, M.; Nishioka, M.; Anzai, S.; Shimoyama, I.; Fukui, K.; Miura, H.; Nakagawa, H.; Nakagawa, K.; Nakagawa, T.; Kinoshita, T. *Solid State Commun.* **1999**, *112*, 91.
(5) Johnson, T. H. *Proc. Soc. Photo-opt. Inst. Eng.* **1984**, *433*, 60.
(6) Willoughby, A. F. W.; Hull, R.; Capper, P. *Widegap II−VI Compunds for Optoelectronic Applications*; Electronic Materials Series; Chapman and Hall: London, 1992; Vol. 1.
(7) Grau, J.; Akinc, M. *J. Am. Ceram. Soc.* **1997**, *80*, 941.
(8) Henshaw, G.; Parkin, I. P.; Shaw, G. A. *J. Chem. Soc., Dalton Trans.* **1997**, 231.
(9) Zhang, X. M.; Wang, C.; Xie, Y.; Qian, Y. T. *Mater. Res. Bull.* **1999**, *34*, 1967.
(10) Xuefeng, O.; Yandong, L.; Yi, X.; Yitai, Q. *Mater. Chem. Phys.* **2000**, *66*, 97.
(11) Meng, Z.; Peng, Y.; Yu, W.; Qian, Y. T. *Mater. Chem. Phys.* **2002**, *74*, 230.
(12) Ghezelbash, A., Jr.; Korgel, B. A. *Nano Lett.* **2004**, *4*, 537.
(13) Chen, D.; Gao, L.; Zhang, P. *Chem. Lett.* **2003**, *32*, 996.
(14) Khiew, P. S.; Huang, N. M.; Radiman, S.; Ahmad, M. D. S. *Mater. Lett.* **2004**, *58*, 762.
(15) Wang, D. Q.; Chen, D. R.; Jiao, X. L. *Chin. Chem. Lett.* **2004**, *15*, 79.
(16) Yu, S.-H.; Yoshimura, M. *Adv. Funct. Mater.* **2002**, *12*, 277.
(17) O' Brien, P.; Park, J. H.; Waters, J. *Thin Solid Films* **2003**, *431*, 502–432.
(18) O'Brien, P.; Waters, J. *Chem. Vap. Deposition* **2006**, *12*, 620.
(19) Cheon, J.; Talaga, D. S.; Zink, J. I. *Chem. Mater.* **1997**, *9*, 1208.
(20) Tiekink, E. R. T.; Haiduc, I. *Prog. Inorg. Chem.* **2005**, *54*, 127.
(21) Koh, Y. W.; Lai, C. S.; Du, A. Y.; Tiekink, E. R. T.; Loh, K. P. *Chem. Mater.* **2003**, *15*, 4544.
(22) Bessergenev, V. G.; Bessergenev, A. V.; Ivanova, E. N.; Kovalevskaya, Y. A. *J. Solid State Chem.* **1998**, *137*, 6.
(23) Barreca, D.; Gasparotto, A.; Maragno, C.; Seraglia, R.; Tondello, E.; Venzo, A.; Krishnan, V.; Bertagnolli, H. *Appl. Organomet. Chem.* **2005**, *19*, 59.

10.1021/cm801330v CCC: $40.75
Published on Web 09/18/2008

Table 1. Crystallographic Data for Compounds 1−5

	1	2	3	4	5
mol formula	$C_{20}H_{28}N_2NiO_2S_4$	$C_{20}H_{26}Br_2N_2NiO_2S_4$	$C_{22}H_{26}N_4NiO_2S_4$	$C_{22}H_{32}N_2NiO_2S_4$	$C_{20}H_{26}Cl_2N_2NiO_2S_4$
fw (g mol^{-1})	515.39	763.20	565.42	543.45	584.28
cryst syst	monoclinic	monoclinic	monoclinic	monoclinic	monoclinic
space group	$P2_1/c$	$P2_1/c$	$P2_1/c$	$C2/c$	$P2_1/a$
a (Å)	11.0733(7)	11.7324(13)	12.4133(6)	16.2821(18)	8.9699(2)
b (Å)	6.0829(4)	12.2907(13)	11.4248(5)	8.8273(10)	12.1472(3)
c (Å)	16.9492(10)	8.9485(10)	9.2350(4)	18.138(2)	11.7178(3)
β (deg)	94.1970(10)	91.866(2)	102.6400(10)	103.902(2)	92.3680(10)
V (Å^3)	1138.60(12)	1289.7(2)	1277.96(10)	2530.6(5)	1275.67(5)
Z	2	2	2	4	2
μ (mm^{-1})	1.238	4.195	1.113	1.118	1.318
ρ (g cm^{-3})	1.503	1.734	1.469	1.426	1.521
θ range (deg)	1.84−30.63	1.74−28.28	1.68−28.27	2.31−28.28	3.27−27.48
R_1, wR_2 [$I > 2\sigma(I)$]	0.0289, 0.0749	0.0229, 0.0601	0.0308, 0.0779	0.0257, 0.0677	0.0315, 0.0708
R_1, wR_2 (all data)	0.0293, 0.0752	0.0244, 0.0610	0.0328, 0.0799	0.0274, 0.0694	0.0442, 0.0761
measured/independent reflns/R	12872/2984/0.0206	13097/3204/0.0365	10673/3165/0.0381	12771/3143/0.0199	16557/2921/0.0535

from a six-membered cyclic transition state. Metal sulfide formation could then occur by subsequent carbonyl sulfide and hydrogen sulfide elimination processes (eq 1).

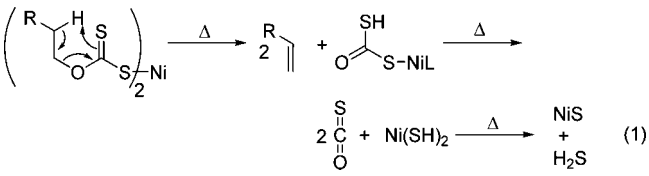

(1)

In this submission, we provide an account of our use of simple bis-pyridine adducts of nickel bis(*O*-*n*-butylxanthate) as remarkably clean single-source precursors for the growth of nickel sulfide thin films by AACVD on glass and ceramic substrates. These latter, six-coordinate compounds offer notable stability and solubility for film growth studies and, *via* the ready substitution of the pyridine ligands, a simple means to effect precise electronic control over decomposition temperature.

2. Experimental Section

All reactions were carried out at room temperature. Reagent-grade solvents were used without further purification. All starting materials were purchased from Sigma Aldrich and used without further purification. The *O*-n-butylxanthate ligand was generated by the reaction between *n*-butanol and CS_2 in the presence of KOH in acetone and crystallized from the same solvent. SEM/EDX and AFM was carried out on a JEOL JSM-6310 microscope, a JEOL JXA-8600 electron probe microanalyzer, and a Veeco Digital Instruments atomic force microscope respectively. XRD was performed using a Bruker D8 diffractometer on which coupled $\theta-2\theta$ scans were carried out. TGA studies were performed on a Perkin-Elmer TGA7 analyzer under a flow of dry N_2 gas. FAB MS (LSSIMS) spectra were recorded on a VG AutoSpec instrument using cesium ion bombardment at 25 kV. Samples were dissolved in a 3-nitrobenzyl alcohol matrix.

Synthesis of Bis(O-*n*-butyldithiocarbonato-κ^2-*S*,*S*′)-bis(pyridine)nickel(II) Complexes, 1−5; Typical Procedure. Potassium *O*-*n*-butylxanthate (1.00 g, 0.53 mmol) was dissolved in acetone (20 mL). $Ni(NO_3)_2 \cdot 6H_2O$ (0.77 g, 0.27 mmol) was added and the green solution stirred for 2 h. At this point the appropriate pyridine (*ca*. 30 mL) was added to give a dark green solution and stirring was continued for a further hour. Filtration and slow evaporation provided high yields (ca. 80%) of the target compounds as green crystals. Elemental anal. (**1**) Found (calcd) for $C_{20}H_{28}N_2NiO_2S_4$: C, 46.61 (46.60); H, 5.47 (5.60); N, 5.43 (5.66). MS (*m*/*z*) 360 ([M − Py + H], 100%). (**2**) Found (calcd) for $C_{20}H_{26}Br_2N_2NiO_2S_4$: C, 35.68 (35.40); H, 3.90 (3.84); N, 4.16 (4.30). MS (*m*/*z*) 360 ([M − Py + H], 100%). (**3**) Found (calcd) for $C_{22}H_{26}N_4NiO_2S_4$: C, 46.73 (46.0); H, 4.64 (4.54); N, 9.91 (9.80). MS (*m*/*z*) 360 ([M − py + H], 100%). (**4**) Found (calcd) for $C_{22}H_{32}N_2NiO_2S_4$: C, 48.62 (48.60); H, 5.95 (5.95); N, 5.16 (5.19). MS (*m*/*z*) 360 ([M − Py + H], 100%). (**5**) Found (calcd) for $C_{20}H_{26}Cl_2N_2NiO_2S_4$: C, 41.00 (41.11); H, 4.52 (4.49); N, 4.70 (4.79). MS (*m*/*z*) 360 ([M − Py + H], 100%).

Pyrolysis of Precursors. Pyrolysis was carried out in a silica boat by heating ca. 0.3 g of each precursor to 450 °C for 1 h in a Carbolite tube furnace under a dinitrogen atmosphere. Upon cooling, the samples were manipulated and transferred for XRD and SEM/EDX analysis without any further protection from the ambient atmosphere.

AACVD. The CVD apparatus consisted of an atmospheric pressure horizontal hot wall reactor containing a silica (1.5 cm diameter) tube heated by a Carbolite tube furnace into which the substrates were placed prior to each deposition run. The nebulizer used consisted of an ultrasonic humidifier from Pifco Health. The ultrasonic transducer transmitted ultrasound through a water reservior and the glass of the flask into the solution to be nebulized. Prior to each deposition, the system was purged with dinitrogen gas and the substrate brought to 300 °C inside the heated silica tube. At this point, the nebulizer was turned on and the mist generated swept out of the flask by a flow of dinitrogen gas (0.3 L min^{-1}) and transported to the reactor chamber. In a typical experiment, 0.4 g of the precursor was dissolved in 15 mL of toluene and delivered to the heated substrate for 2 h.

X-ray Crystallography. Crystallographic data for compounds **1**−**5** are displayed in Table 1. Data collections were implemented either on a Bruker AXS SMART APEX CCD (**1**−**4**) at 100 K or a Nonius KappaCCD (**5**) diffractometer at 150 K. All non-hydrogen atoms were refined anisotropically. Refinement was based on F^2 against all reflections. All hydrogen atoms were placed in calculated positions and refined isotropically with a displacement parameter 1.5 (methyl) or 1.2 (all others) times that of the adjacent carbon atom. In compound **4**, the sulfur-containing ligand was disordered over two positions in a 1:1 ratio because of an interaction of one of the sulfur atoms with the methylene moiety of C10, resulting in an alteration of the orientation of CH_2 groups in neighboring molecules.

3. Results and Discussion

The five representative bis(*O*-*n*-butyldithiocarbonato-κ^2-*S*,*S*′)bis(pyridine)nickel(II) precursor complexes, [Ni($S_2CO^nBu)_2 \cdot (C_5H_5N)_2$] (**1**), [Ni($S_2CO^nBu)_2 \cdot (3-Br-C_5H_4N)_2$]

Table 2. Selected Bond Lengths (Å) and Angles (deg) for Compounds 1−5

	1[a]	**2**[b]	**3**[c]	**4**[d,e]	**5**[b]
Ni−N(1)	2.0887(11)	2.1021(13)	2.1095(13)	2.1052(10)	2.1085(16)
Ni−S(1)	2.4319(3)	2.4426(4)	2.4401(3)	2.456(5)	2.4377(4)
Ni−S(2)	2.5004(3)	2.4628(4)	2.4264(4)	2.445(3)	2.4593(5)
N(1)−Ni−N(1)′	180.00(3)	180.0	180.0	180.0	180.0
N(1)−Ni−S(1)	90.59(3)	89.50(4)	90.00(3)	91.00(11)	90.37(4)
N(1)−Ni−S(2)	90.05(3)	89.66(4)	91.02(3)	88.69(9)	90.56(4)
S(1)−Ni−S(2)	73.188(10)	73.722(12)	74.557(11)	73.71(9)	73.886(15)
S(1)−Ni−S(2)′	106.812(10)	106.280(12)	105.444(11)	106.29(9)	106.114(15)

[a] Symmetry transformation to generate equivalent atoms: $-x + 2, -y, -z$. [b] Symmetry transformation to generate equivalent atoms: $-x + 1, -y + 1, -z + 1$. [c] Symmetry transformation to generate equivalent atoms: $-x + 2, -y, -z + 2$. [d] Symmetry transformation to generate equivalent atoms: $-x + 1/2, -y + 5/2, -z$. [e] Measurements refer to S(1A) and S(2A) of disordered ligands.

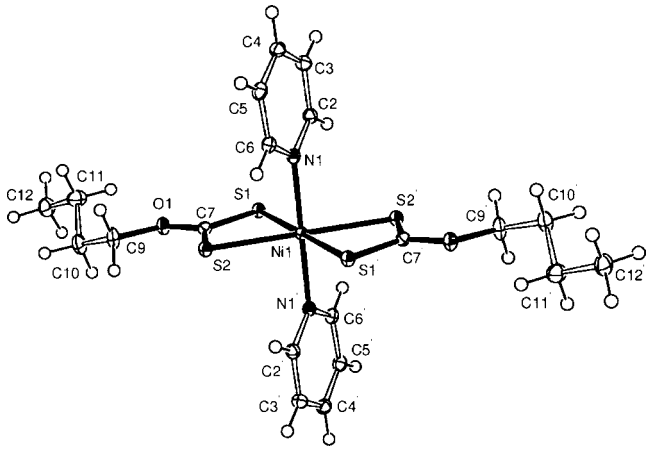

Figure 1. ORTEP representation of compound **1** (30% probability level ellipsoids).

(**2**), $[Ni(S_2CO^nBu)_2(4\text{-}CN\text{-}C_5H_4N)_2]$ (**3**), $[Ni(S_2CO^nBu)_2\cdot(3\text{-}Me\text{-}C_5H_4N)_2]$ (**4**), and $[Ni(S_2CO^nBu)_2\cdot(3\text{-}Cl\text{-}C_5H_4N)_2$ (**5**), were readily synthesized by metathesis of the potassium *O*-*n*-butylxanthate with nickel(II) nitrate in acetone and addition of the appropriately substituted pyridine, as green compounds after crystallization from the same solvent. All five compounds have been characterized by elemental analysis and single-crystal X-ray diffraction analysis and **1**−**4** by thermogravimetric analysis (TGA). Details of the X-ray analyses are provided in Table 1. Although selected bond length and angle data for all five compounds are provided in Table 2, only the representative structure of compound **1** is illustrated in Figure 1. Although **1**−**5** are not isostructural, in all five compounds the Ni atom is located on a center of inversion and exists within a six-coordinate *trans*-N_2S_4 donor set. Any deviations from an octahedral geometry are necessarily enforced by the bite angle of the bidentate κ^2-S_2CO^nBu ligands (S(1)−Ni−S(2), *ca*. 74°), which are somewhat narrower than those typically observed in nickel(II) dithiocarbamates such as $[Ni(S_2CNMe^nBu)_2]$ (79.2°).[18] The remaining bond lengths and angles are entirely typical of those observed in previous structurally characterized nickel xanthate complexes,[24−26] such as the similarly six-coordinate bis(*O*-benzylxanthate) complex $[Ni(S_2COCH_2Ph)_2(NC_5H_3\text{-}Me\text{-}3)_2]$,[24] with essentially invariant Ni−S bond distances.

TGA performed on compounds **1**−**4** up to 500 °C demonstrated the onset of very rapid mass loss at temperatures >100 °C for all four compounds. In all four cases, the thermal decomposition appears to be a two-stage process (Figure 2). For compounds **1**, **2**, and **4**, the first stage was essentially complete at *ca*. 170 °C and resulted in mass losses of 69, 78, and 66% respectively. The 4-cyanopyridine adduct, compound **3**, although displaying a similar two-stage decomposition, was more thermally stable and required heating to 200° before the cessation of the initial rapid 76% weight loss. Regardless of any variability in the thermal stability of the complexes, it is notable that the percentage mass loss in this low temperature step is, in all four cases, effectively commensurate with the formation of a common nickel dithiocarbonate intermediate, $[NiCS_2O]$, consistent with a decomposition reaction driven by loss of the adducted pyridine molecules prior to the aforementioned Chugaev/COS/H_2S elimination sequence (eq 1). In all four cases, further heating to temperatures in excess of 500 °C accounted for a more gradual weight loss of carbonyl sulfide and H_2S, leaving residues of **1**, 19% (NiS requires 17.6%); **2**, 13% (NiS requires 13.5%); **3**, 18% (NiS requires 17.6%); and **4**, 17% (NiS requires 16.7%). It is notable that these temperatures are generally significantly lower than those required by related dithiocarbamate-based chemistries.[17,18] Prompted by these results, pyrolysis of each precursor was carried out at 450 °C in a static tube furnace under a flow of dinitrogen. In each case, XRD analysis (Figure 3) of the resultant black powders identified the presence of rhombohedral NiS (Millerite, JCPDS 75−0612) as the predominant crystalline phase present in each of the black residues, albeit with some evidence for the likely presence of $NiS_{1.03}$ indicated by the low intensity peak at 46° in 2θ.

Examination by energy-dispersive X-ray (EDX) analysis of these residues also provided evidence for the purity of the samples and revealed emission due exclusively to nickel and sulfur atoms within the detection limits of the experiment.

The relatively low decomposition temperatures and inherently low volatility of compounds **1**−**4** mitigated against their use as precursors to thin film NiS by conventional low pressure chemical vapor deposition. As a consequence of their good solubility in common organic solvents, however, AACVD was identified as a viable option for vapor-phase transport. Compounds **1**−**4** were dissolved in toluene, nebulized, and delivered to the substrates by a dinitrogen carrier gas flow (0.3 L min^{-1}) over a period of 2.0 h. Although the TGA studies indicated an optimal formation of NiS at 350 °C, attempted deposition at this temperature produced excessive prereaction and the formation of non-

(24) Campian, M.; Haiduc, I.; Tiekink, E. R. T *Acta Crystallogr., Sect. E* **2006**, *62*, m3516.
(25) Travnicek, Z.; Pastorek, R.; Sindelar, Z.; Klicka, R.; Marek, J. *Polyhedron* **1995**, *14*, 3627.
(26) Xu, K.; Ding, W.; Meng, W.; Hu, F. *J. Coord. Chem.* **2003**, *56*, 797.

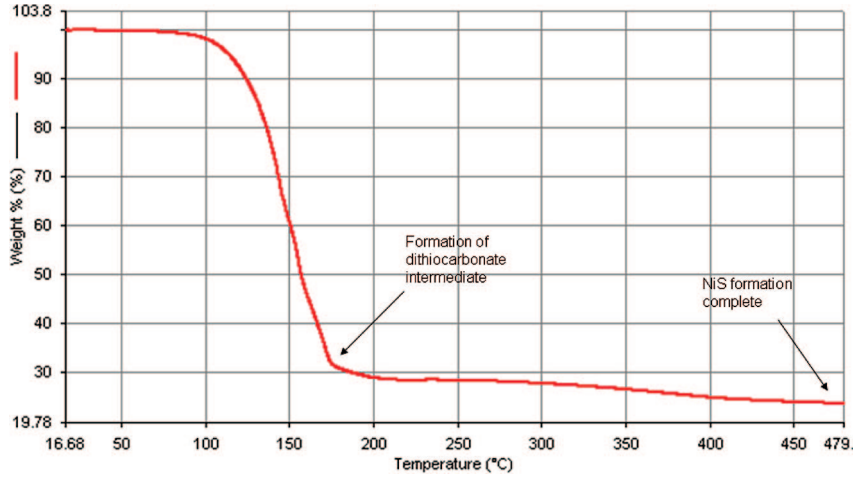

Figure 2. TGA trace for the thermal decomposition of compound **1**.

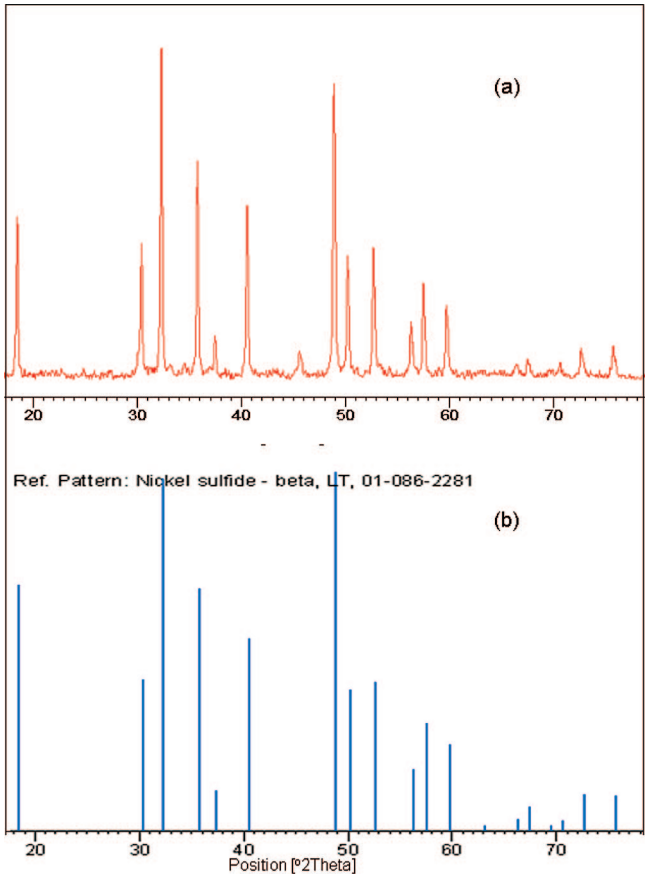

Figure 3. (a) XRD pattern of NiS obtained by pyrolysis of compound **1**; (b) reference pattern for Millerite (JPCDS 75−0612).

adhesive powdery deposits on the substrate surfaces. Deposition under nebulized conditions at 300 °C, however, typically produced contiguous black metallic films with a golden luster that adhered well with good coverage of the substrate surface. Despite the use of several different substrates (bare glass, SnO_2-coated glass, and TiO_2-coated glass and porous ceramic), the exact nature of the surface appeared to have little effect upon the deposited films in terms of appearance to the naked eye and coverage. Although films deposited under these conditions were too thin for definitive analysis, extension of the deposition period to 6 h allowed for the growth of suitably thick films, which glancing angle XRD analysis identified rhombohedral (Millerite) NiS as the only crystalline nickel sulfide phase (Figure 4). Notably no contamination by $NiS_{1.03}$, as had been apparent in the bulk pyrolysis studies, was observed in the thin film materials, possibly as a result of the reduced (300 versus 350 °C) temperature of preparation. Subsequent annealing of these films to 500 °C produced no apparent change to the crystallinity or crystalline composition of the deposited films.

Interestingly, repetition of the experiments under these conditions employing chloroform rather than toluene as solvent resulted in the codeposition of an additional phase, which EDX results suggested contained chloride. Although this line of enquiry has not been further explored in this study, this observation indicates that the current methodology may also provide a potential route to alternative materials compositions *via* judicious selection of an appropriately reactive solvent medium. SEM analysis of the thin films grown direct onto soda lime glass revealed a densely packed florettelike morphology with individual formations of the order of 1−4 μm across. Images a and b in Figure 5 illustrate typical films deposited from compounds **3** and **4**, respectively.

In contrast, films deposited from toluene solution onto crystalline metal oxide-coated surfaces (TiO_2 or SnO_2) displayed a more regular appearance as densely packed platelike crystallites which were oriented perpendicular to (TiO_2, Figure 6a) or coplanar with (SnO_2, Figure 6b) the substrate surface. The microscopic appearance of films deposited onto ceramic substrates displayed a similarly contiguous and finely grained consistency (Figure 6b) for all four precursors. These observations contrast quite markedly from previous studies of NiS deposition (LPCVD or AACVD conditions) employing nickel dithiocarbamato precursors, $[Ni(S_2CNRR')_2]$, which were observed to be composed of either nanowires or heaped globular formations depending upon the precise identity of the precursor and the deposition temperature.[17,18]

Despite this substrate-dependent variation in morphology, qualitative EDX analysis detected nickel and sulfur as the only elements present other than the constituent elements present in the substrates. Further information about film particle size, surface roughness and morphology was obtained

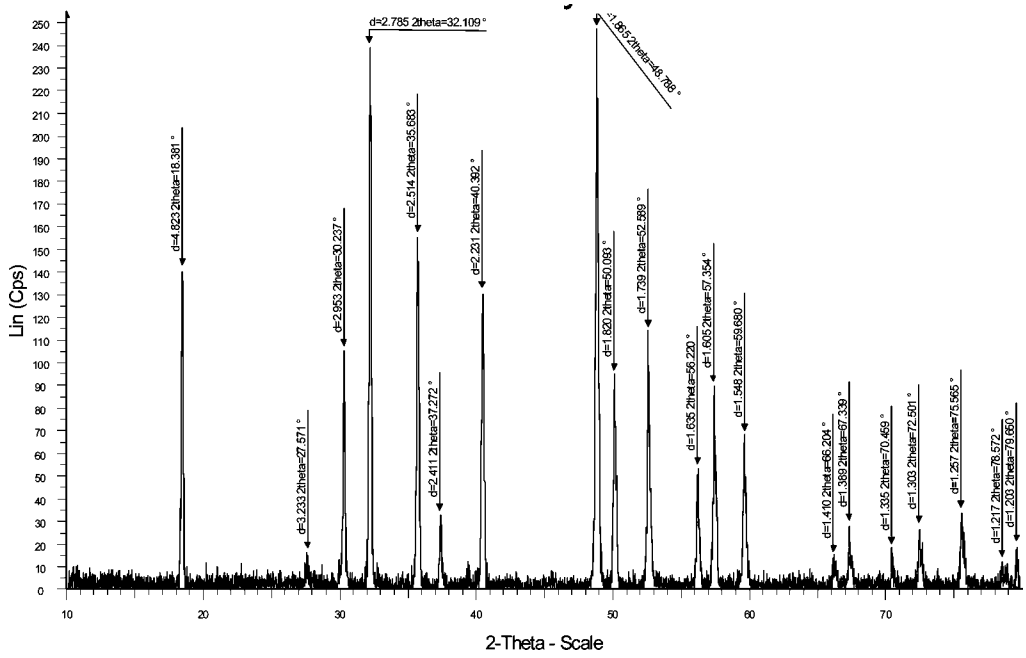

Figure 4. XRD pattern of film deposited by the AACVD of compound **1** onto bare glass at 350 °C.

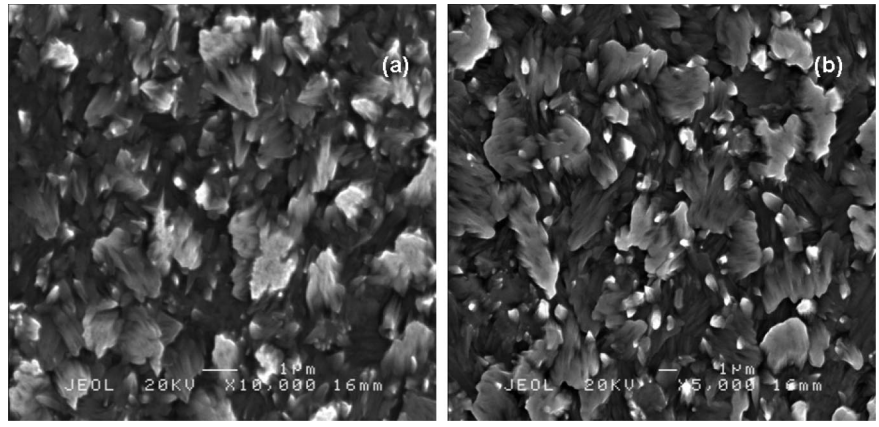

Figure 5. SEM images of films deposited on bare glass by the AACVD of (a) compound **3**, (b) compound **4**.

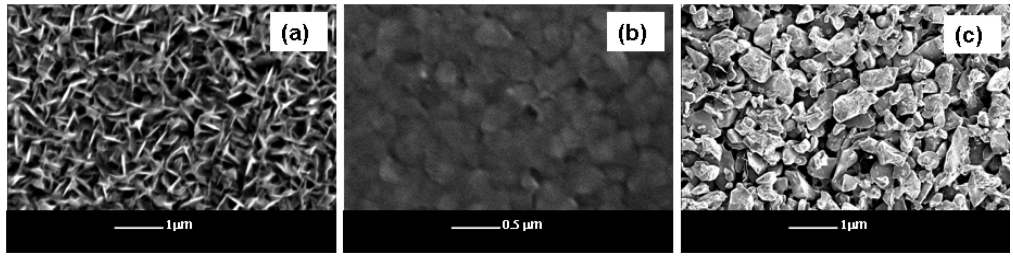

Figure 6. SEM images of films deposited on bare glass by the AACVD of compound **1** onto (a) TiO_2, (b) SnO_2, and (c) ceramic substrates.

from atomic force microscopy (AFM) measurements performed upon selected films deposited onto each of the representative substrates. Figure 7 illustrates a typical output provided by this analysis obtained from a representative film employing deposition of compound **1** onto a glass substrate.

This analysis provided an average particle size of ca. 58−60 nm^2 and an rms surface roughness of ca. 300−350 Å regardless of the identity of the NiS precursor employed and, by means of a section analysis of a deliberately applied scratch, an estimation of a typical growth rate achieved under the conditions of the deposition. This latter analysis indicted that the pure NiS films were of the order of 3000 Å thick, providing a growth rate of some 1500 Å h^{-1}.

4. Conclusions

In summary, this contribution reports the use of an easily synthesized series of nickel *O*-*n*-butylxanthate bis(pyridine) adducts as clean precursors to crystalline NiS thin films under very mild AACVD conditions. Although minor variations in the precise morphology of the films has been noted to display a dependence upon the precise nature of the substrate

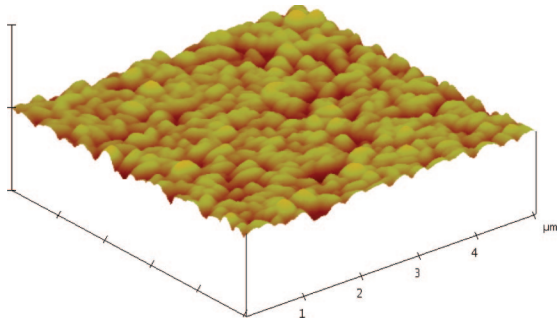

Figure 7. Typical AFM image of film deposited on bare glass by the AACVD of compound **1**.

surface, the composition of the as-deposited films was consistent across all of the precursors studied, despite some minor variations in compound thermal stability. We are continuing to study this chemistry and related applications of **1**−**5** in nanoparticle synthesis where such simply introduced variability in precursor stability may be best suited to provide a means of subtle control over particle size and structure.

Acknowledgment. Mr Alan Carver at the University of Bath is thanked for elemental analyses and Mr. Hugh Perrott of the Department of Materials at the University of Bath is thanked for assistance with SEM, EDX, and AFM measurements. The Royal Society is thanked for the provision of a University Research Fellowship (M.S.H.) and the Higher Education Council (HEC) of Pakistan for a 6 month postgraduate fellowship (N.A.).

Supporting Information Available: Crystallographic information for the single-crystal X-ray studies of compounds **1**−**5**. This material is available free of charge via the Internet at http://pubs.acs.org.

CM801330V